

# Experimental study on the evaporating progress of hexane lens on immiscible liquid: Spreading and receding

*Aiqiang CHEN<sup>1,2</sup>, Jinghong YIN<sup>1,2</sup>, Huiqin WANG<sup>1,2</sup>, Bin LIU<sup>1,2,\*</sup>, Rachid BENNACER<sup>1,3</sup>*

<sup>1</sup>Tianjin Key Laboratory of Refrigeration Technology, Tianjin University of Commerce, Tianjin, 300134, China

<sup>2</sup>International Centre in Fundamental and Engineering Thermophysics, Tianjin University of Commerce, Tianjin, 300134, China

<sup>3</sup>LMT/ENS-Cachan/CNRS, Paris-Saclay University, 61 Avenue du Président Wilson, 94235 Cachan, France

\*Corresponding author: [lbtjcu@tjcu.edu.cn](mailto:lbtjcu@tjcu.edu.cn) Tel: +86 189 2019 7448

**Abstract:** The change of evaporation liquid on another immiscible liquid has important guiding significance for many applications. In this experiment, the geometric temperature distribution and evaporation rate of n-hexane droplets were observed and recorded by changing the temperature of deionized water. The results show that with the increase of temperature of deionized water-based solution, the maximum diameter of n-hexane droplet spreading after titration increases gradually, while the minimum diameter of n-hexane droplet disappearing decreases gradually. Meanwhile, the evaporation rate of n-hexane droplet is constant during the whole evaporation process. It should also be mentioned that if the base solution is changed from deionized water to a certain concentration of salt solution, the maximum diameter of n-hexane droplet spreading will be reduced, and the evaporation intensity will be relatively reduced. These experimental results will give us a better understanding of the mechanism and characteristics of droplet evaporation.

**Keywords:** Water, Temperature, Hexane, Lens, Evaporating progress, Surface tension

## 1. Introduction

Droplet evaporation is a common phenomenon in nature. It is of great significance to study it. Many scholars have conducted in-depth and extensive research on droplet evaporation, and literature [1] and [2] have made a detailed summary of the research in this aspect. The evaporation of liquid droplets is one of the research aspects, but the evolution of an evaporating droplets on a nonmiscible liquid

substrate has only recently received attention, which is of practical importance in many industrial occasion<sup>[3]</sup>. According to the different application scenarios, the research can be divided into several aspects, such as the separation and fusion of droplets on the liquid surface<sup>[4-6]</sup>, the impact of droplets on the liquid surface<sup>[7-11]</sup>, the Leighton frost effect on the liquid surface<sup>[12]</sup>, and the geometry and evolution of droplets attached to the liquid surface.

When the liquid drops on the surface of the insoluble liquid, there are three possibilities: complete wetting, partial wetting, and pseudopartial wetting, actually occurs is governed by competition between long- and short-range

forces, the latter two states are often referred to as "Lens". In the early stage of lens research, we focused on the theoretical analysis and measurement methods of lens geometry. Based on the Young–Laplace equation, Neumann's rule is constructed to describe the geometry of lens. When an alkane lens is placed on the surface of a surfactant solution, its three-phase contact line has an associated line tension, which plays a crucial role in determining the relative size<sup>[13]</sup>. Pujado et al. analyzed the effect of line tension at the three-phase line of lens on liquid surface, and constructed an approximate calculation method for the geometric structure of lens considering this factor<sup>[14]</sup>. Emelyanenko et al. established the three-phase contact angle calculation formula of benzene lens based on the isoline of separation pressure. It was found that the spreading and shrinking process of benzene lens was the result of several different types of surface forces, among which the moisture content of benzene lens had a greater influence<sup>[15]</sup>. Ooi et al. studied the floating mechanism of lens by CT scanning technology. It was found that the shape of lens was mainly affected by the surface tension, and the contact angle would change with the volume of lens due to the flexibility of the base liquid interface<sup>[16]</sup>. Burton et al. developed a Mathematica program based on Young–Laplace equation to analyze lens geometry of liquid<sup>[17]</sup>, and this lens profile calculator, together with a measurement of the lens radius for a known volume, provides a simple and convenient method of determining the spreading coefficient (S) of a liquid lens system. Nikolov et al. also reviewed the related research of liquid lens, proposed an accurate method to measure the three-phase contact angle of micro lens by using reflected light interference, verified the effectiveness of Neumann rule for micro lens, and evaluated the three-phase contact angle and the radius of upper and lower interfaces of two kinds of (spreading and non spreading) lens<sup>[3]</sup>.

Another focus on the study of liquid lens is its dynamic dissolution, spreading and evaporation process. Kim et al. studied the mixing mechanism of miscible liquid, and found that the lens structure and Marangoni convection can also be produced before the miscible liquid is mixed, and established a theoretical model to predict its spreading time, geometric scale and Marangoni convection velocity<sup>[18]</sup>.

Keiser et al. studied the instability of lens (water + ethanol) formed by the mixed solution of water and ethanol on sunflower oil surface, and found that the wetting transition at the three-phase line and Marangoni effect caused by rapid evaporation of ethanol both led to the diffusion and fragmentation of lens<sup>[19]</sup>. Nosoko et al. studied the evaporation process of n-pentane lens on water surface, and found that the static time of water, the purity of n-pentane, the temperature difference of environment and other factors can significantly affect the evaporation time and geometric characteristics<sup>[20]</sup>. Shimizu et al. studied the evaporation process of n-pentane and trifluoroacetyl chloride droplets on water surface under moderately elevated pressures (0.48 MPa), and Data obtained were processed to yield information on parameters of practical importance<sup>[21]</sup>. Gelderblom et al. studied the evaporation process of small droplets on the liquid surface, and revealed the flow law in the three-phase contact line region by solving Stokes equation<sup>[22]</sup>. Sun et al. Studied the evaporation process of toluene and n-hexane lens on the deionized water surface, and found that both of them experienced the spreading stage and the shrinking stage in turn, and the shrinking speed increased significantly when the dimensionless time was 0.7 ~ 0.8<sup>[23]</sup>. Phan et al. Studied the floatability of water droplets on the oil surface, and found that the stability of floating droplets is affected by the interfacial tension between various media, oil density and water droplet volume. The water droplets are more stable after adding surfactant, which indicates that the surfactant plays an important role in the stability of water droplets<sup>[24]</sup>. Bresme et al. used molecular dynamics method to simulate the wetting behavior of nanoscale liquid lens on the liquid interface, and found that Neumann rule in the macro scene can also accurately describe the wetting behavior of nanoscale lens<sup>[26]</sup>. Bertrand et al. measured the wetting behavior of different alkanes on water surface by ellipsometry, and found that there were two wetting transitions of alkanes. Based on the experimental data, the wetting transition function with alkane chain length and temperature as variables was constructed<sup>[27]</sup>.

As mentioned above, although many scholars have done a lot of research on this topic, compared with other fields, the research in this field is obviously insufficient, so there are still many problems and phenomena that need to be explored and explained. Because the liquid base liquid

surface is flexible and variable, and the droplet is "convex lens", the internal flow characteristics and the stability of the three-phase line during the evaporation of volatile lens on the liquid surface are determined by the base liquid and the droplet. The internal flow characteristics of volatile lens, the instability mechanism and dynamic evolution of three-phase line region need to be further explored. Therefore, the evaporation process of n-hexane droplet on the surface of deionized water and NaCl solution with different concentrations was observed experimentally. The diameter evolution of n-hexane lens, the change of evaporation rate and the instability at the three-phase line were recorded. The variation of evaporation rate of n-hexane lens in evaporation process was analyzed, and the instability mechanism of three-phase line of n-hexane lens was discussed. The relevant conclusions can provide reference for the follow-up scientific research and process design.

## 2. Materials and methods

### 2.1 Experimental apparatus

The experimental data involved in this paper are measured by three relatively independent experimental devices, including real-time image measurement system, surface temperature measurement system and evaporation rate measurement system. The real-time image acquisition system consists of a 3D video microscope (rh2000, hirox, Japan), a computer, a micro feeding pump and a culture dish. The 3D video microscope is connected with the computer to transmit the collected image to the computer. The diameter of the culture dish is XX mm and the depth is XX mm. In order to ensure the accuracy of titration volume and the experimental requirements, the syringe is equipped with a 250 mm long metal probe.

The surface temperature measurement system is

composed of infrared thermal imager (x6520, FLIR, USA), computer, culture dish, micro feeding pump, thermocouple and data recorder. Among them, the resolution of the infrared thermograph is 640×512 and the temperature resolution is 0.05k, two T-type thermocouples are used, which are connected with data recorder. The thermocouples are calibrated carefully ( $\pm 0.1^{\circ}\text{C}$ ) before use, and inserted into the medium of culture dish to monitor the temperature change of medium.

The evaporation rate measurement system is composed of high precision electronic balance, computer, lens, culture dish, micro liquid pump, thermocouple and data recorder. The culture dish is placed on the tray inside the high-precision electronic balance. The high-precision balance is connected with the computer, and the quality reading is directly imported into the computer for recording.

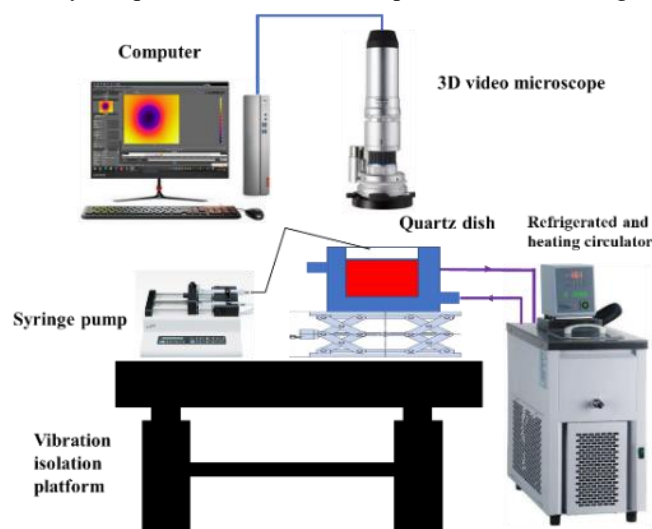


**Figure 1.** Schematic of the experimental setup for the evaporation of a hexane lens on the surface of immiscible liquid.

### 2.2 Experimental materials

Deionized water was used as the base liquid, which was produced by an ultrapure water apparatus (UPT-11-20T, ULUPURE, China). Hexane (purity:  $> 99\%$ , Shanghai Macklin Biochemical Co. Ltd. China) is chosen as the experimental material, which is water-insoluble and volatile.

The NaCl used for preparing salt solution was purchased from (purity: > 99.8%, Shanghai Macklin Biochemical Co. Ltd. China). High precision electronic balance was used to weigh NaCl and deionized water, and salt solutions with mass fractions of 6%, 12%, 18% and 24% were prepared and put in closed containers for standby.

## 2.3 Experimental procedure

Before the experiment, most of the dust and dirt on the surface of syringe, culture dish and thermocouple probe were removed by ultrasonic cleaning instrument, and then cleaned with acetone, alcohol and distilled water in turn one after another, for five minutes each, followed by air flow treatment for drying.

During the experiment, the container containing the base solution was put into a constant temperature water bath and heated or cooled to a specific temperature (Table 1). The heated or cooled base solution was poured into the culture dish (15mm deep). The temperature change of the base solution was monitored by thermocouple. When the base solution temperature reached the set temperature, the temperature of the base solution was measured by the thermocouple, a hexane droplet of 2  $\mu\text{L}$  was titrated on the surface of base solution via the syringe pump, leading to the formation of a lens. The 3D video microscope was used to record the image change of the droplet during the evaporation process from top, a digital electronic balance (auw220d, Shimadzu, Japan) was used to measure the mass change during evaporation. Each experiment was repeated 6 times. The room temperature remained at  $21 \pm 1$  °C, and the relative humidity remained in the range 30%~40%.

## 2.4 Data processing

The diameter change of n-hexane lens during evaporation

was obtained by Image J software. The video file of n-hexane lens evaporation process recorded by 3D video microscope was imported into image J, and the change of n-hexane lens diameter with time was measured by using the measurement function of the software. The evaporation rate of n-hexane is equal to the mass change rate of n-hexane droplet (n-hexane lens + base solution) minus the mass change rate before n-hexane is added.

## 3. Results

### 3.1 Characteristics of droplet spreading and diameter variation

When n-hexane droplets are exposed to salt solutions at different temperatures (concentration: 18%), the diameter change of n-hexane lens is shown in Fig. 2a. We can find that the change of the diameter of n-hexane lens can be divided into three stages: 1) spreading stage, which is similar to the change of droplet shape on the solid plane. In this stage, the diameter of n-hexane increases rapidly from the initial diameter under the action of gravity and interfacial tension. When the three-phase contact line reaches the force balance, the diameter of n-hexane lens reaches the maximum; 2) In the contraction stage, the diameter of n-hexane decreases continuously in this stage. It should be noted that in this stage, the diameter of n-hexane lens decreases at a constant rate (stage I) and increases suddenly at a certain time (stage II); 3) in the instant disappearance stage, the diameter of n-hexane does not decrease continuously to 0, but decreases continuously to a certain value. When it reaches a certain value, the lens structure of n-hexane collapses suddenly and Lens

disappears. The diameter of NS becomes "zero", and the original lens spreads out into several liquid membranes. The diameter and evaporation time of n-hexane lens were dimensionless treated at different base solution temperatures. The results are shown in Fig. 2B. It can be found that the evolution pattern of the diameter of n-hexane lens is very similar at different base liquid temperatures. When the dimensionless excess time is about 0.1, the diameter of n-hexane lens reaches the maximum, and the diameter of n-hexane lens begins to decrease linearly from 0.2. When the dimensionless excess time is about 0.8, the decrease rate of lens diameter increases, which indicates that the evaporation process of n-hexane has changed significantly.

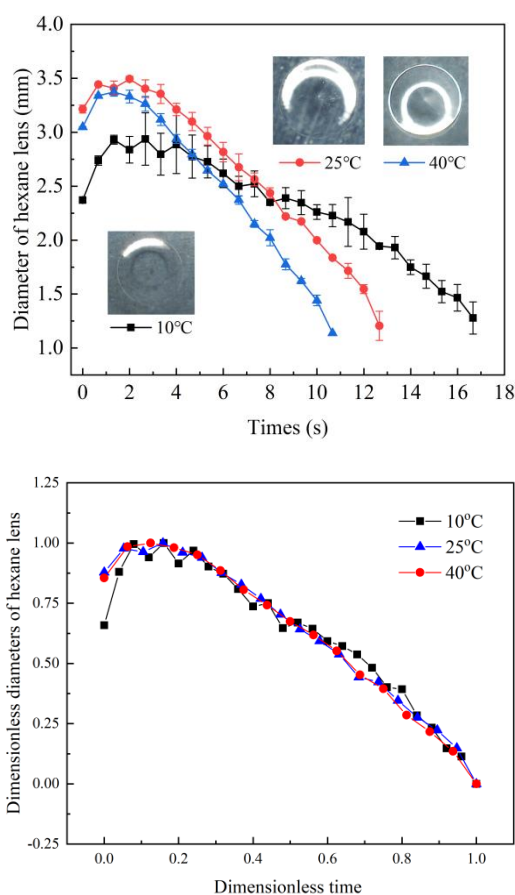


**Figure.2** Diameters variation of hexane lens (2ul) with time.

When the temperature of base solution is different, the diameter of n-hexane lens shows different evolution rules. Compared with the salt solution temperature of 25°C and 40°C, the initial diameter of n-hexane lens on the surface of 10°C salt solution is 2.371 mm, while the initial diameter of

n-hexane lens on the surface of 10°C salt solution is 3.215 mm and 3.05 mm when the salt solution temperature is set at 25°C and 40°C. When the base solution temperature is 10°C, the maximum diameter of n-hexane is 2.94 mm, which is also significantly lower than that of the salt solution temperature of 25°C and 40°C. When the salt solution temperature is 10°C, the average decreasing rate of the diameter of n-hexane lens is 0.115 mm / s, which is significantly lower than that of deionized water temperature of 25°C (0.2158 mm / s) and 40°C (0.2563 mm / s). By dimensionless treatment of the diameter of n-hexane lens at three salt solution temperatures, we can find that there is no significant difference in the evaporation mode among them. Another important phenomenon is still worthy of our attention. When the temperature of deionized water is different, the final diameter of n-hexane in the form of lens is significantly different. When the temperature of deionized water is 10°C, 25°C and 40°C, the corresponding diameters of n-hexane lens are 1.278 mm, 1.2055 mm and 1.138 mm, respectively. The lower the temperature of deionized water is, the larger the diameter of final disappearance is. The higher the temperature of deionized water is, the smaller the diameter of final disappearance is.

The overall mass change of n-hexane in the spreading and evaporation process of deionized water on the salt solution base solution at different temperatures is shown in Figure 2. The whole mass change is composed of two parts, one is the evaporation of base solution, the other is the evaporation of n-hexane. After adding n-hexane droplets, the overall mass has a small increase in a short period. After reaching equilibrium, the mass begins to decrease gradually. At this time, the decrease of overall mass is the common result of n-hexane evaporation and base liquid evaporation. It is easy to see that the overall quality of the two plants decreased linearly, indicating that the overall evaporation rate did not change. After a period of time, the overall mass change rate has a significant change. At this time, n-hexane has evaporated completely, and the mass loss is only caused by the evaporation of base solution. The evaporation rate of n-hexane can be obtained by subtracting the evaporation rate of falling section 3 from the evaporation rate of stage 2. As the total mass of stage 2 and stage 3 changes linearly, we can infer that the evaporation rate of n-hexane is relatively constant in the whole process, that is, the volume reduction

rate of n-hexane lens remains unchanged.

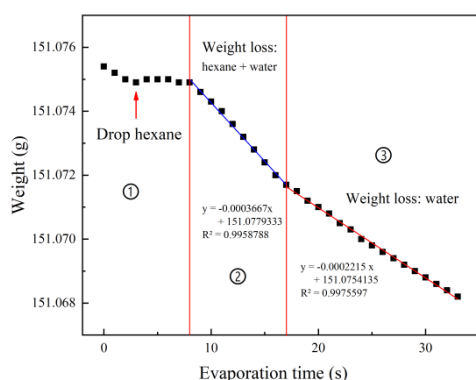


**Fig. 3** mass change of n-hexane during evaporation from salt solution at different temperatures

### 3.2 Effect of salt solution concentration on n-hexane evaporation process

When the temperature of base solution remains unchanged (25°C), and the concentration of salt solution is 0%, 6%, 12%, 18% and 24%, the diameter change of n-hexane is shown in Fig. 3. The diameter change of n-hexane lens also experienced spreading stage, linear shrinkage stage and transient disappearance stage. When the base solution is salt solution, the maximum diameter of n-hexane after spreading is significantly larger than that when the base solution is deionized water. However, the diameter and change trend of n-hexane lens did not show significant difference with the change of salt solution concentration, that is, the presence of NaCl changed the geometry of n-hexane lens, but the change of NaCl solution concentration did not have a significant effect. In particular, it should be noted that the evaporation time of n-hexane lens in different concentrations of salt solution is 47.03s, 48.89s, 48.9 and

46.9s respectively, while when the base solution is deionized water, the evaporation time of the same volume of n-hexane lens is 37.15s, which shows that the evaporation intensity of n-hexane lens decreases when the base solution is salt solution. When the concentration of n-hexane is different, the corresponding diameters of n-hexane lens structure collapse are 1.424mm (0%), 1.413mm (6%), 1.59mm (12%), 1.49mm (18%) and 1.55mm (24%), respectively. The critical diameters of n-hexane structure collapse on different concentration of n-hexane solution at the same temperature have little difference.

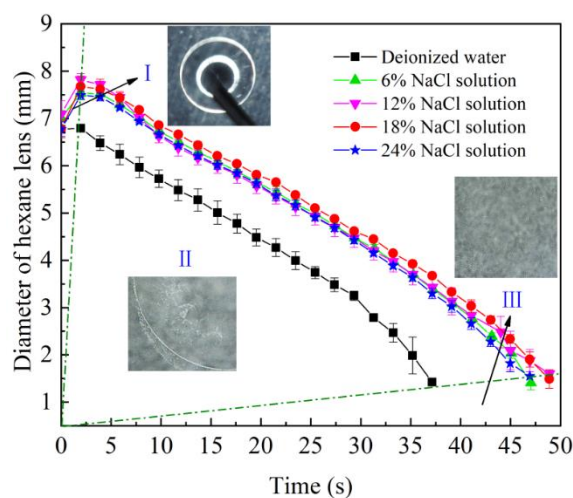


**Fig.4** diameter change of n-hexane droplet on the surface of different concentration salt solution (initial volume 6ul)

### 3.3 Evolution of lens trilinear in n-hexane

The morphology and evolution of n-hexane lens will change with the evaporation process, and each stage shows different characteristics (Fig. 5). In the spreading stage, n-hexane first contacts with the base solution. The main characteristics of this stage are that the flow from the center to the edge is very obvious at the moment when n-hexane contacts with the base solution, and n-hexane lens gradually spreads out. When the force at the lens three-phase contact line reaches

equilibrium, the diameter of n-hexane does not continue to increase. Then the lens of n-hexane entered into the linear contraction stage and showed some new characteristics. N-hexane can be divided into three regions (Fig. 5): edge instability region, middle vortex region and central sinking reflux region. In the edge instability region, n-hexane forms many tiny "droplets" at the boundary, which fall off from the edge of n-hexane and gradually diffuse outward. In addition, the region of micro droplets on the boundary is not uniform, and the velocity of micro droplets away from n-hexane is also different.

There is a significant flow from the boundary to the center in the upper part of n-hexane lens. The vortex starts from a certain area inside the three-phase line of n-hexane lens. The geometric thickness near the three-phase contact line is small, so the vortex cannot extend into this area. Next to the region is the region where eddy current is generated and affected.

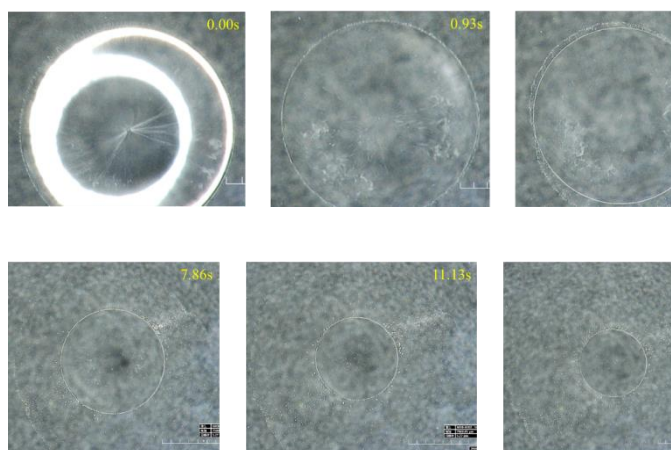


**Figure.5** shows the characteristics of small droplets in this region

The n-hexane vortex flows along the surface of n-hexane from the edge to the center of n-hexane. When approaching the center, the flow turns to the inside of n-hexane. However, when the diameter of n-hexane decreases to a certain critical value, a new significant change occurs: 1) the reduction rate of n-hexane diameter increases significantly (Fig. 5F), which can also be seen from Fig. 2 and Fig. 3 It was observed that: 2) the diameter of micro droplets produced at the edge was significantly reduced (Fig.

5g). When the diameter decreases to a critical value, the lens structure of n-hexane disintegrates instantaneously and a thin film is formed. After evaporation, all the small droplets and films will remain on the surface of deionized water, and finally form three distinct areas, as shown in Fig. 6.

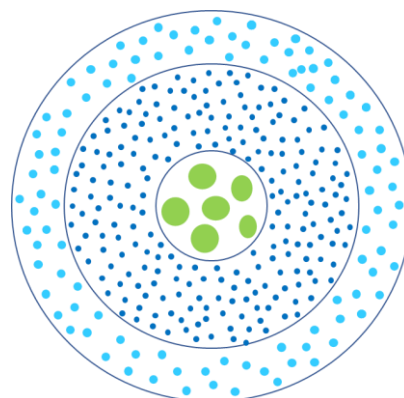


**Fig. 6** characteristics and distribution of residual droplets

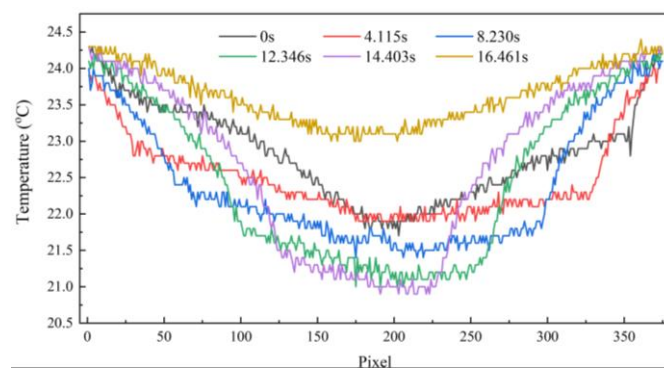


**Fig. 7** Variation of surface temperature of n-hexane with time during evaporation

## 4 Discussion

For a system consisting of hexane and DI water or NaCl solution, both  $S$  and  $A$  are positive, and pseudopartial wetting is expected. In the experiments by bgil, K. [28], hexane droplets on the surface of fresh DI water remained the shape of liquid lenses during both the advancing and receding stages in an environment with unsaturated hexane vapor.

## 4.1 Reasons for the difference of n-hexane diameter

In most cases, the surface tension will gradually decrease with the increase of temperature. However, we fitted the surface tension of deionized water and n-hexane with the change of temperature between 0°C and 5°C, and found that the change rates of surface tension of deionized water and n-hexane with the change of temperature were -0.1525mn/m°C and -0.1062mn/m°C, respectively. Therefore, the influence of the temperature of deionized water on the geometry of n-hexane is greater than that of n-hexane. According to Neumann's law, the larger the surface tension of deionized water is, the larger the diameter of lens is. The maximum spreading diameter of n-hexane is  $d(10^\circ\text{C}) > d(25^\circ\text{C}) > d(40^\circ\text{C})$ . However, the maximum spreading diameter of n-hexane lens at 10°C is significantly smaller than that at 25°C and 40°C, indicating that the maximum spreading diameter of n-hexane lens is also affected by other factors. Re examining Figure 4, it can be seen that n-hexane rapidly forms many tiny droplets during contact, and the spreading diameter of lens formed by n-hexane is not only affected by the surface (boundary) tension, but also affected by the dynamic drop off condition. The diameter of n-hexane lens is caused by volume reduction, and the volume loss is caused by evaporation and

Both the contact angles and the radius of droplet shedding.

the liquid lens play important roles in the variation of the resultant force and the motion of the contact line. The largest receding rate at the end of the lifetime of a liquid lens is also associated with the fast evaporation due to the formation of a thin-disk lens with a small radius.

The diameter of n-hexane lens is closely related to its volume and contact angle. The droplet volume is determined by two aspects: one is the evaporation process, the other is the separation of tiny droplets in the boundary region. Following the work given by Sun and Yang<sup>[29]</sup>, the resultant force,  $\Delta F$ , applied to the contact line can be expressed as

$$\Delta F = \gamma_1 \cos \theta_1 + \gamma_2 \cos \theta_2 - \gamma_1 - \eta \frac{dx}{dt}$$

## 4.2 Reasons for linear variation of evaporation rate

It can be seen from Figure 3 that the mass of n-hexane lens decreases linearly, indicating that the evaporation rate of n-hexane is relatively constant. Generally, the evaporation process of droplets can be described by Fick's law, the hexane lens starts to evaluate due to the difference of hexane concentration between the surface of the lens and the air, which can be described by Eq. (1).

$$\dot{m} = -M_w A_w k_c \left( \frac{p_s(T_w)}{RT_w} - \frac{p_v}{RT_a} \right) \quad (1)$$

where,  $\dot{m}$  is the evaporation rate of hexane lens, g/s;  $A_w$  is the surface area of droplet, m<sup>2</sup>;  $M_w$  denotes the molecular weight of hexane, g/mol;  $C_{w,s}$ ,  $C_{w,\infty}$  denotes the vapor concentration on the surface of droplet and in the air, respectively, mol/m<sup>3</sup>;  $T_w$  and  $T_a$  are the surface temperature of the lens and the temperature of air, respectively, K;  $p$  is the local absolute pressure, Pa;  $R$  is the universal gas constant, 8.3145 J/(mol·K).

Therefore, if the evaporation process of n-hexane lens conforms to Fick's law, the two phenomena seem to be contradictory, and the evaporation rate should gradually decrease, which is inconsistent with the experimental results. Let's revisit Fick's law, which describes droplet evaporation. Because the experiment is carried out in an open environment and the ambient temperature is constant. Therefore,  $D_\infty$  can be considered as a constant.  $DS$  is directly related to temperature. The temperature change during evaporation is observed by infrared thermal imager. The surface temperature of n-hexane during evaporation

changes with time, as shown in Figure 7. It can be found that the surface temperature of n-hexane decreases with the evaporation process.

$k_c$  denotes the mass transfer coefficient, kg/s, which can be obtained from the Sherwood number correlation as follows,

$$Sh = \frac{k_c d_w}{D_c} = 2 + 0.6 Re^{\frac{1}{2}} Sc^{\frac{1}{3}} \quad (2)$$

$$Sc = \frac{\nu}{D_c} \quad (3)$$

$$Re = \frac{\rho_w d_w u_d}{\mu} \quad (4)$$

where  $d_w$  is the diameter of droplet, m;  $Sc$  is the Schmidt number;  $Re$  is the Reynolds number;  $D_c$  is the diffusion coefficient of hexane vapor in the air, m<sup>2</sup>/s;  $u_d$  is the velocity of droplet, m/s.

### 4.3 Influence of salt solution concentration

The diameter of n-hexane in different concentration of salt solution has little difference, but the diameter of lens in deionized water and salt solution has great difference. At the same base solution temperature, although the diameter of n-hexane on deionized water of salt solution and deionized water is quite different, the dimensionless diameter shows that there is no essential difference in evaporation mode between them. The geometry of n-hexane on the two base solutions is the key factor affecting the evaporation rate, which is determined by the temperature itself and the lens of n-hexane. The surface tension of salt solution increases with the increase of salt concentration, so the diameter of n-hexane should increase gradually with the increase of salt concentration. However, the data show that the presence of NaCl has a significant effect, while the concentration of base solution has no obvious effect.

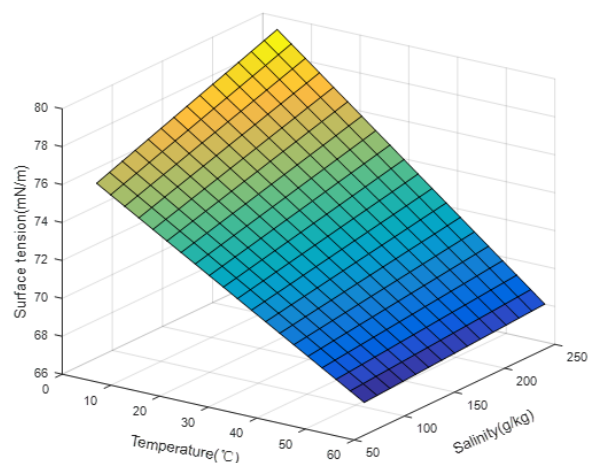


Fig. 8 Effect of salt solution concentration on n-hexane diameter

### 4.4 Principle of three phase line instability

The surface temperature of deionized water and n-hexane lens are different, so we can't calculate them according to the same temperature. This process is a dynamic balance rather than a static force balance process.

The reason why the instability of lens three-phase system can occur may be due to the flow. At this time, the surface tension size at the three-phase line has a problem, which may change the surface tension distribution.

The development and evolution of convective patterns induced by evaporation is a complex problem. For a volatile fluid, the vertical temperature gradient results from the evaporation itself and from the coupling between the free surface and the surroundings. If the temperature decrease is large enough, buoyancy forces and surface tension variations may overcome stabilizing forces, and convection begins<sup>[30]</sup>.

## 5. Conclusions and Prospect

We found that the change of the diameter of n-hexane lens can be divided into three stages: 1) spreading stage; 2) shrinkage stage; 3) instant disappearance stage. The initial diameter and maximum diameter of n-hexane lens begin to increase with the increase of base solution temperature, and then decrease with the increase of base solution temperature after reaching a certain peak value. When n-hexane lens was added to the base solution, the evaporation rate of the whole solution increased, and when n-hexane evaporated, the solution returned to the original evaporation rate of the base solution. When the base solution is salt solution, the evaporation rate of n-hexane lens increases with the increase of salt solution concentration.

In any case, lens has good research prospects and research value. After all, lens phenomenon occurs in all aspects of life. I hope my research can make us better understand lens phenomenon itself, so as to have a clearer understanding of lens application in the future.

## Acknowledgements

This work was financially supported by the Tianjin Natural Science Foundation (N° 18JCQNJC84600), the Foundation of Tianjin Educational Committee (N° 2017KJ177).

## Reference

1. D. Brutin, Droplet Wetting and Evaporation, Academic Press, San Diego, 2015.
2. D. Zang, S. Tarafdar, Y.Y. Tarasevich, M. Dutta Choudhury, T. Dutta, Evaporation of a Droplet: From physics to applications, Physics Reports, 804 (2019) 1-56.

3. A. Nikolov, D. Wasan, Oil lenses on the air–water surface and the validity of Neumann's rule, Adv Colloid Interfac, 244 (2017) 174-183.
4. F. Blanchette, L. Messio, J.W.M. Bush, B. A., R. E., The influence of surface tension gradients on drop coalescence  
Decay of standing foams: Drainage, coalescence and collapse, Phys Fluids, 21 (7) (2009) 072107.
5. T.S. T., T. K., The coalescence cascade of a drop, Phys. Fluids, 12 (2000) 1265.
6. X. Cheng, Y. Zhu, Z. Lei, D. Zhang, K. Tao, Numerical analysis of deposition frequency for successive droplets coalescence dynamics, Phys Fluids, 30 (4) (2018) 042102.
7. M. Kumar, R. Bhardwaj, K.C. Sahu, Coalescence dynamics of a droplet on a sessile droplet, Phys Fluids, 32 (1) (2020) 012104.
8. B. Wang, C. Wang, Y. Yu, X. Chen, Spreading and penetration of a micro-sized water droplet impacting onto oil layers, Phys Fluids, 32 (1) (2020) 012003.
9. X. Tang, A. Saha, C.K. Law, C. Sun, Bouncing drop on liquid film: Dynamics of interfacial gas layer, Phys Fluids, 31 (1) (2019) 013304.
10. N.E. Ersoy, M. Eslamian, Capillary surface wave formation and mixing of miscible liquids during droplet impact onto a liquid film, Phys Fluids, 31 (1) (2019) 012107.
11. Z. Che, O.K. Matar, Impact of droplets on immiscible liquid films, Soft Matter, 14 (9) (2018) 1540-1551.
12. E. Mogilevskiy, Levitation of a nonboiling droplet over hot liquid bath, Phys Fluids, 32 (1) (2020) 012114.
13. P.A. Ash, C.D. Bain, H. Matsubara, Wetting in oil/water/surfactant systems, Curr Opin Colloid In, 17 (4) (2012) 196-204.
14. P. Pujado, L. Scriven, Sessile lenticular configurations: translationally and rotationally

- symmetric lenses, *J Colloid Interf Sci*, 40 (1) (1972) 82-98.
15. K.A. Emelyanenko, A.M. Emelyanenko, L.B. Boinovich, Spreading and contraction of a benzene lens on water: A description on the basis of the disjoining pressure, *Colloids and Surfaces A: Physicochemical and Engineering Aspects*, 522 (2017) 601-607.
16. C.H. Ooi, C. Plackowski, A.V. Nguyen, R.K. Vadivelu, J.A.S. John, D.V. Dao, N.-T. Nguyen, Floating mechanism of a small liquid marble, *Sci Rep-Uk*, 6 (2016) 21777.
17. J. Burton, F. Huisman, P. Alison, D. Rogerson, P. Taborek, Experimental and numerical investigation of the equilibrium geometry of liquid lenses, *Langmuir*, 26 (19) (2010) 15316-15324.
18. H. Kim, K. Muller, O. Shardt, S. Afkhami, H.A. Stone, Solutal Marangoni flows of miscible liquids drive transport without surface contamination, *Nature Physics*, 13 (11) (2017) 1105-1110.
19. L. Keiser, H. Bense, P. Colinet, J. Bico, E. Reyssat, Marangoni Bursting: Evaporation-Induced Emulsification of Binary Mixtures on a Liquid Layer, *Phys.rev.lett*, 118 (7) (2017) 074504.
20. T. Nosoko, T. Ohyama, Y. Mori, Evaporation of volatile-liquid lenses floating on an immiscible-liquid surface: effects of the surface age and fluid purities in n-pentane/water system, *J Fluid Mech*, 161 (1985) 329-346.
21. Y. Shimizu, Y.H. Mori, Evaporation of single liquid drops in an immiscible liquid at elevated pressures: experimental study with n-pentane and R 113 drops in water, *Int J Heat Mass Tran*, 31 (9) (1988) 1843-1851.
22. H. Gelderblom, H.A. Stone, J.H. Snoeijer, Stokes flow in a drop evaporating from a liquid subphase, *Phys Fluids*, 25 (10) (2013) 102102.
23. W. Sun, F. Yang, Evaporation of a volatile liquid lens on the surface of an immiscible liquid, *Langmuir*, 32 (24) (2016) 6058-6067.
24. C.M. Phan, B. Allen, L.B. Peters, T.N. Le, M.O. Tade, Can water float on oil?, *Langmuir*, 28 (10) (2012) 4609-4613.
25. C.M. Phan, Stability of a floating water droplet on an oil surface, *Langmuir*, 30 (3) (2014) 768-773.
26. F. Bresme, N. Quirke, Computer simulation studies of liquid lenses at a liquid-liquid interface, *The Journal of Chemical Physics*, 112 (13) (2000) 5985-5990.
27. E. Bertrand, H. Dobbs, D. Broseta, J. Indekeu, D. Bonn, J. Meunier, First-Order and Critical Wetting of Alkanes on Water, *Phys Rev Lett*, 85 (6) (2000) 1282-1285.
28. K. Ragil, D. Bonn, D. Broseta, J. Indekeu, F. Kalaydjian, J. Meunier, The wetting behavior of alkanes on water, *J Petrol Sci Eng*, 20 (3) (1998) 177-183.
29. H. Kim, J. Lee, T.H. Kim, H.Y. Kim, Spontaneous Marangoni Mixing of Miscible Liquids at a Liquid-Liquid-Air Contact Line, *Langmuir the Acs Journal of Surfaces & Colloids*, (2015) 150731094843008.
30. G. Toussaint, H. Bodiguel, F. Doumenc, B. Guerrier, C. Allain, Experimental characterization of buoyancy- and surface tension-driven convection during the drying of a polymer solution, *Int J Heat Mass Tran*, 51 (17) (2008) 4228-4237.